ECE measurements in WENDELSTEIN 7-X plasmas

M. Hirsch[1], J. Geiger[1], H.-J. Hartfuss[1], U. Höfel[1,2], F. Köster[1,2], H. Maaßberg[1], N. B. Marushchenko[1], S. Schmuck[3], T. Stange[1], J. Svensson[1], H. Tsuchiya[4], G. M. Weir[1], R. C. Wolf[1] and the W7-X Team

[1] *Max-Planck-Institut für Plasmaphysik, Greifswald, Germany*
[2] *Zentrum für Astronomie und Astrophysik, Technische Universität Berlin*
[3] *Culham Science Centre, Abingdon, OX14 3DB, United Kingdom*
[4] *National Institute for Fusion Science, Toki, Japan*

The optimized stellarator Wendelstein 7-X aims at ECRH-heated high-density steady-state discharges at reactor relevant collisionality regimes and beta. During its first operation phase, OP1.1, dedicated to integrated commissioning, tests of components and diagnostics, the device was equipped with five uncooled inboard carbon limiters, which restricted the magnetic configuration. To avoid uncontrolled overheating the overall energy input for a single experiment scenario had been set to < 4MJ. For the maximum available heating power, P_{ECRH}= 4 MW provided by 6 gyrotrons, these conditions allowed a discharge duration of 1.2s, equivalently a stationary discharge of 6s could be realized at reduced power.

1. Electron Cyclotron Emission Diagnostic

The Electron Cyclotron Emission diagnostic, ECE, was operated throughout OP1.1 as the main tool to study electron heating by ECRH and the subsequent electron heat transport. It measures the 2nd harmonic X-mode emission (X2) in the frequency band from 126 GHz to 162 GHz with a 32-channel heterodyne radiometer located outside the torus hall [1]. The sightline is defined by in-vessel Gaussian optics with beam width w_0 < 30 mm throughout the plasma. The sightline is oriented perpendicular to the stellarator flux surfaces to minimize refraction and Doppler broadening and to maximize the radial resolution by minimizing the emitting volume. The polarization of the probed radiation is defined by the fundamental waveguide at the output of the microwave horn antenna inside the vessel. Microwave stray radiation resulting from non-absorbed power of the various gyrotrons in the frequency band (139.9 to 140.4 GHz) is cut out of the spectrum by a waveguide Bragg reflection notch filter with a depth >40 dB showing extremely steep edges and an insertion loss of 3 to 5 dB outside this frequency band [2]. This radiometer is supplemented by an additional 16 channel "zoom system" in parallel to the standard filterbank that measures a 4GHz wide frequency span by the aid of a tunable second Local Oscillator which allows the selection of any frequency range of the spectrum. The selected range corresponds to Δr~6cm at the High-Field Side

(HFS) or ~15cm at the Low Field Side (LFS). The radiometer is absolutely calibrated by a second, identical Gaussian optical system as a twin outside the torus including identical waveguide components, mica window and a geometrically identical transmission line, however, with a hot-cold calibration source chopping between LN_2 temperature and room temperature at its aperture. Relative calibration of both optics in the laboratory has been taken into account and showed an accuracy of 5%, provided spurious reflections in the transmission path are carefully avoided. The overall absolute calibration error is estimated to be ~10% with outliers for individual channels due to low detection sensitivity.

2. ECE spectra and temperature profiles

As an example, Fig.1 shows selected ECE time traces together with other discharge parameters for an experiment scenario with ECRH power levels at 2 MW and 0.8 MW at nearly stationary density of ndl=2.5 10^{19} m^{-2}, i.e. n = 1.9 10^{19} m^{-3}. At densities beyond this, the discharge could not be maintained but was terminated by radiation [4]. The ECE channels display quasi stationary conditions for the different phases reaching central temperatures of 7 keV and 5 keV, respectively. Ion temperatures reaching about 2 keV increase almost steadily all over the discharge due to the only moderate electron-ion coupling.

ECE spectra measured at the times marked in Fig.1 show that besides the X2 emission, which is attributed to blackbody radiation from thermal electrons along the sightline, further components occur: for the lowest frequencies on the LFS (positive r_{eff}) the ECE spectra show the well known downshifted emission from higher-energetic thermal electrons in the plasma center for which the plasma is optically grey. This is confirmed from the temporal behavior of this spectral feature during plasma start-up and -termination as well as from its parameter dependency. Ray tracing calculations to model the spectrum using the TRAVIS code [3], which applies a fully-relativistic model of EC-absorption and -+emission, indicate that the relevant emitting thermal electrons in the core have an energy of E~$3 \cdot k_B T$. Furthermore, for the rather low densities and strong on-axis ECRH, the ECE spectrum on its low field side displays a shoulder that resembles a contribution which seems to be on top of the blackbody emission representing the electron temperature. This contribution disappears faster than the emission from the thermal bulk when the ECRH is switched off (compare green and red spectrum) or when switching from on- to off-axis heating (not shown in this example).

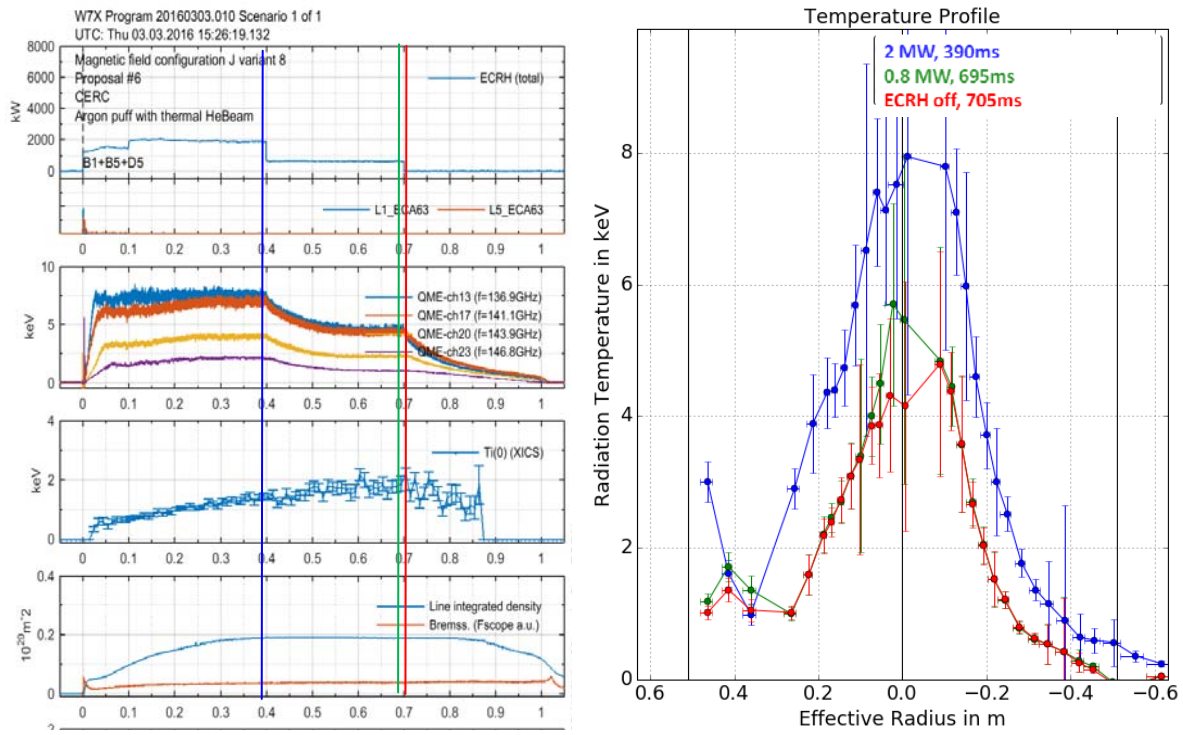

Fig.1: Left: Waveforms (from top to bottom) of ECRH heating power, selected ECE radiometer channels on the high field side, central T_i derived from X-ray imaging spectroscopy [5] together with the line integrated density (blue) [6] and Bremsstrahlen (red), for a discharge with power steps. Right: The ECE emission profiles shown, integrated over 5ms each, are selected at 390 ms (blue, 2 MW ECRH), 690ms (green, 0.8 MW ECRH) and 702ms (red, right after ECRH has been terminated).

T_e-profiles are derived from the X2 emission spectra taking into account the finite optical thickness via the ray-tracing code TRAVIS [3,7]. The ECE blackbody emission displays those electrons that are located at the ECE sightline behind the cold resonance with a typical shift, which for the T_e and n_e profiles obtained in OP1.1 can be approximated by $\Delta L = 3\text{mm} + 2\text{mm/keV} \cdot T_e(\text{keV})$ in real space. First comparison with T_e-profiles obtained from Thomson scattering [8] and imaging X-ray spectroscopy [5] yield good agreement for most discharges [9]. In summary, for the low density hydrogen limiter plasmas obtained in OP1.1 electron temperatures can be maintained stationary until the heating is terminated with discharge lengths up to 6s. Profiles of on-axis heated plasmas show a hot core surrounded by steep electron temperature gradients at around half of the minor radius resembling core electron-root conditions [12]. In general, the T_e-profiles are highly reproducible for the same conditions and broaden considerably with off-axis heating, i.e. there is no indication for profile stiffness in the plasma center yet.

3. Dynamic transport studies

The ECE radiometer displays a variety of dynamic plasma phenomena such as mode activity [7,10] and individual transport events. The zoom device with its radially close channels also allowed for first temperature fluctuation studies using radial correlation techniques [7]. A nearly coherent activity with frequency around 7 to 10 kHz is visible in ECE channels located ~r/a=0.5 in several scenarios. Mirnov coil measurements show an m=5 mode rotating in the electron diamagnetic direction possibly related to an $\iota = 4/5$ rational surface [10,13]. An example of crash events associated with strong off-axis heating is shown in Fig.2.

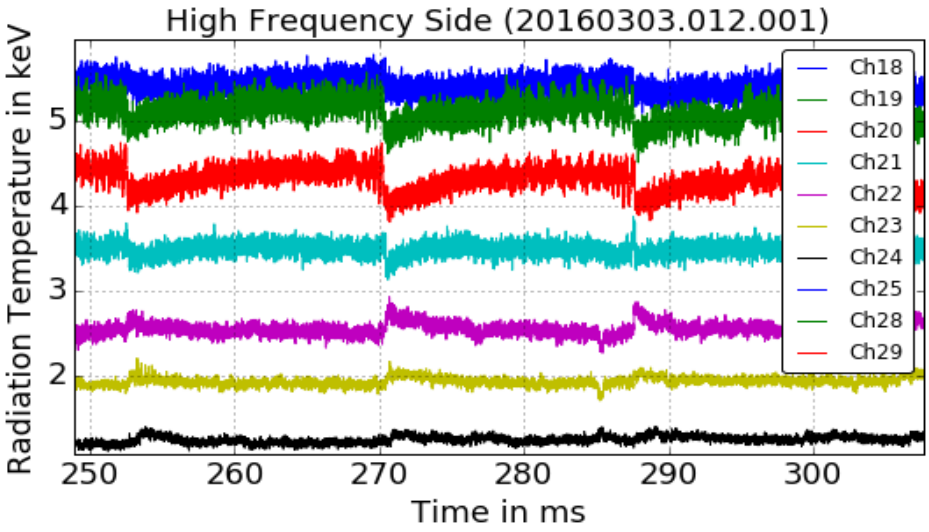

Fig.2: Te-crashes with precursor oscillations during *off-axis* ECRH. Inversion radius at r_{eff}=0.20m.

Stationary and dynamic transport studies were conducted together with the flexible ECRH system with its option for on- and off-axis heating, power steps and power modulation. Heatwave propagation experiments, with on- and off-axis power modulation of the gyrotrons, allow for the determination of the ECRH power deposition profiles as well as for dynamic electron transport studies that are presented in [11].

Aknowledgement

This work has been carried out within the framework of the EUROfusion Consortium and has received funding from the Euratom research and training programme 2014-2018 under grant agreement No 633053. The views and opinions expressed herein do not necessarily reflect those of the European Commission.

References:

[1] Hirsch M et al. 2015, Proceedings of Science, *1st ECPD, April 2015, Villa Mondragone , Frascati (Italy)*
[2] Wagner D. *et al.* 2011 *J Infrared Milli Terraherz Waves* **32** 1424–1433
[3] Marushchenko N et al 2014 Computer Phys. Commun. 185(1) 165-176
This conference: [4] Zhang D et al (P4-015), [5] Langenberg A et al (P4-014), [6] Knauer J et al (P4.017), [7] Weir G et al (P4.009), [8] Pasch et al (P4.016), [9] Bozhenkov et al (O2.106), [10] Rahbarnia et al (P4.011), [11] Höfel et al (P4.008), [12] Dinklage et al (O2.107), [13] Thomsen et al (P4.010).